

Reduced Capillary Length Scale in the Application of Ostwald Ripening Theory to the Coarsening of Charged Colloidal Crystals in Electrolyte Solutions

Jeffrey D. Rowe · James K. Baird

Published online: 15 August 2007
© Springer Science+Business Media, LLC 2007

Abstract A colloidal crystal suspended in an electrolyte solution will ordinarily exchange ions with the surrounding solution and develop a net surface charge density and a corresponding double layer. The interfacial tension of the charged surface has contributions arising from: (a) background interfacial tension of the uncharged surface, (b) the entropy associated with the adsorption of ions on the surface, and (c) the polarizing effect of the electrostatic field within the double layer. The adsorption and polarization effects make negative contributions to the surface free energy and serve to reduce the interfacial tension below the value to be expected for the uncharged surface. The diminished interfacial tension leads to a reduced capillary length scale. According to the Ostwald ripening theory of particle coarsening, the reduced capillary length will cause the solute supersaturation to decay more rapidly and the colloidal particles to be smaller in size and greater in number than in the absence of the double layer. Although the length scale for coarsening should be little affected in the case of inorganic colloids, such as AgI, it should be greatly reduced in the case of suspensions of protein crystals, such as apoferritin, catalase, and thaumatin.

Keywords Capillary length · Double layer · Ostwald ripening · Proteins · Silver iodide

J. D. Rowe · J. K. Baird
Department of Physics, University of Alabama in Huntsville, Huntsville, AL 35899, USA

J. K. Baird (✉)
Department of Chemistry, University of Alabama in Huntsville, Huntsville, AL 35899, USA
e-mail: jkbaird@matsci.uah.edu

1 Introduction

A colloidal crystal suspended in an electrolyte solution will ordinarily exchange ions with the solution and develop a net surface charge density [1]. This surface charge is the source of an electric field that acts on the ions in the surrounding solution to create a polarized ion plasma. The combination of the adsorbed charges on the crystal and the displaced ions in the solution phase is termed a *double layer*. The free energy of the surface plus the double layer contains contributions from: (a) the crystal surface entropy associated with the mixing of empty sites with occupied sites containing adsorbed ions [2], (b) the electrostatic energy stored in the polarized ion plasma [2,3], and (c) the change in aqueous solution entropy caused by the demixing of ions of opposite sign under the action of the electric field [3].

The interfacial tension, $\gamma(\sigma)$, of a surface with charge density, σ , in contact with an electrolyte solution can be calculated by evaluating the formula [2–4],

$$\gamma(\sigma) = \gamma_0 + \Gamma_S k_B T \ln(1 - \theta(\sigma)) - \int_0^\phi \sigma(\phi') d\phi' \quad (1)$$

In Eq. 1, γ_0 is the interfacial tension of the *uncharged* surface, ϕ is the electrostatic potential of the *charged* surface, Γ_S is the total density of ion adsorbing sites on the *uncharged* surface, and $\theta(\sigma)$ is the fraction of those sites ionized. The remaining symbols are Boltzmann's constant, k_B , and the temperature, T .

The second term on the right-hand side of Eq. 1 represents the chemical free energy associated with the mixing of empty and occupied adsorption sites on the crystal surface. The third term includes the free energy stored in the plasma electric field, plus the effect of the entropy change associated with the demixing of ions in the aqueous phase [3]. The second and third terms can be omitted in the case of an *uncharged* surface [4]. The second term can be omitted in the case of a *charged* surface when the chemical potential of the ion species being exchanged between the solution and the surface is identical to the chemical potential of this ion species in the bulk solid. Substances satisfying this latter criterion include metals and sparingly soluble salts and metal oxides [3]. The third term on the right-hand side of Eq. 1 is negative, as is the second term, since $\theta(\sigma) < 1$. Hence, the net effect of the formation of the double layer is to lower the interfacial tension of the *charged* surface below the value characteristic of the *uncharged* surface. The reduced interfacial tension will manifest itself in any surface phenomenon in which a double layer is involved. Examples include static phenomena, such as electrocapillarity [5], and dynamic phenomena, such as crystallization [5]. We will consider one aspect of the latter.

From a theoretical point of view, the mechanism of crystallization of a solute from a supersaturated solution is ordinarily divided into sequential stages [6]: (a) *nucleation*, in which molecules aggregate to form embryos (or nuclei) either within the parent phase or on the surface of a substrate, (b) *growth*, where mature nuclei evolve into crystals that advance in size, and (c) *coarsening*, in which large crystals grow at the expense of smaller crystals.

Below, we shall examine, the role of reduced interfacial tension in the theory of coarsening. We will find that the direct effect is to decrease the capillary length scale that governs the time scale as well as the average particle size. We can expect, among the observable consequences of reduced capillary length that the decay of the supersaturation should be faster and the crystals should be smaller in size and greater in number than would be the case in the absence of the double layer.

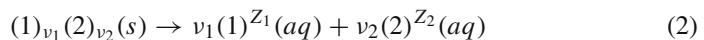
2 Theory

2.1 Role of Coarsening in the Crystallization Process

Although a separation of the mechanism of crystallization into sequential stages is convenient from a theoretical point of view, the individual stages can be expected to overlap to some degree in practice. Nuclei will continue to form while, more mature crystals are already growing. Due to the relentless increase in the total mass of the solid precipitate, however, the solute supersaturation in the solution phase will decay monotonically. Since the solubility of a solid particle decreases as its size increases [7], nuclei and small crystals will dissolve, when it happens that their individual solubilities are above the ambient solute concentration. This will cause the nucleation rate to subside and the phase transition to be taken over by the process of coarsening. In the Ostwald ripening picture of coarsening, the larger crystals will grow at the expense of the smaller crystals, and the total number of crystals will diminish. The process of Ostwald ripening will terminate in principle with one crystal left in equilibrium with the solution at a solute concentration equal to the bulk solubility of the solid [6].

2.2 Size Dependence of the Solubility of a Charged Colloidal Particle

In order to develop a quantitative picture of the effect of surface charge density on the coarsening process, we shall begin by considering a particle of a solid with chemical formula, $(1)_{\nu_1}(2)_{\nu_2}$, that dissolves by electrolytic dissociation,



In Eq. 2, $(1)^{Z_1}(aq)$ is a cation with valence, Z_1 , and $(2)^{Z_2}(aq)$ is an anion with valence, Z_2 . The respective stoichiometric coefficients are ν_1 and ν_2 . The solid phase is denoted by s , while the aqueous phase is denoted by aq . The chemical potential, $\mu(aq)$, of a dissociated molecule of this electrolyte is given by [8]

$$\mu(aq) = \mu^\circ(aq) + \omega k_B T \ln(\gamma_{\pm} Q m) \quad (3)$$

where $\mu^\circ(aq)$ is the chemical potential evaluated in the solute standard state and m is the number of moles of the electrolyte dissolved per kilogram of solvent. Both $\omega = \nu_1 + \nu_2$ and $Q = (\nu_1^{\nu_1} \nu_2^{\nu_2})^{1/\omega}$ are pure numbers that involve only the stoichiometric coefficients. The activity coefficients of the individual ion species, γ_i ($i = 1, 2$), have been combined to define the geometric mean activity coefficient, $\gamma_{\pm} = (\gamma_1^{\nu_1} \gamma_2^{\nu_2})^{1/\omega}$.

We shall assume that the solid phase, represented by the left-hand side of Eq. 2, exists in the form of a colloidal particle of radius, a . In the Kelvin approximation, the Gibbs free energy of the solid is then given by [9]

$$G(s) = n\mu^o(s) + \gamma(a)A \quad (4)$$

In Eq. 4, n is the number of molecules in the particle, $\mu^o(s)$ is the chemical potential of a molecule in the bulk solid, $A = 4\pi a^2$ is the surface area of the particle, and $\gamma(a)$ is the interfacial tension, which we assume is a function of the particle radius, a . The chemical potential, $\mu(s)$, of a molecule in the particle, including the effects of the surface, can be obtained by differentiating Eq. 4 with respect to n . If we introduce the particle volume, $V = (4\pi/3)a^3$, the molecular volume, $v = dV/dn$, and compute $da/dV = 1/4\pi a^2$, then the chemical potential, $\mu(s) = \partial G(s)/\partial n$, can be written as

$$\mu(s) = \mu^o(s) + v \left[\frac{2\gamma(a)}{a} + \frac{d\gamma(a)}{da} \right] \quad (5)$$

The requirement that the solute in the solution and the material in the precipitated phase be in equilibrium is $\mu(aq) = \mu(s)$. Using Eqs. 3 and 5, this criterion can be expressed in the form,

$$\mu^o(aq) + \omega k_B T \ln(\gamma_{\pm} Qm(a)) = \mu^o(s) + v \left[\frac{2\gamma(a)}{a} + \frac{d\gamma(a)}{da} \right] \quad (6)$$

In Eq. 6, we have recognized that the solubility of the particle, $m(a)$, is a function of the radius. If we can also assume that $\lim_{a \rightarrow \infty} (\gamma(a)/a) = \lim_{a \rightarrow \infty} (d\gamma(a)/da) = 0$, then in the limit of large radius, Eq. 6 becomes

$$\mu^o(aq) + \omega k_B T \ln(\gamma_{\pm} Qm(\infty)) = \mu^o(s) \quad (7)$$

where $m(\infty)$ corresponds to the solubility of the bulk solid. The value of the geometric mean activity coefficient, γ_{\pm} , depends upon the ionic strength of the solution [8]. If the ionic strength is sufficiently low as to make the value of γ_{\pm} essentially unity, or if the ionic strength has been fixed by addition of inert electrolyte in sufficient excess to make γ_{\pm} constant, then we can eliminate γ_{\pm} by subtraction of Eq. 7 from Eq. 6 to obtain

$$\omega k_B T \ln \left(\frac{m(a)}{m(\infty)} \right) = v \left[\frac{2\gamma(a)}{a} + \frac{d\gamma(a)}{da} \right] \quad (8)$$

Equation 8 is a generalized Gibbs–Kelvin equation, which is also sometimes termed a Gibbs–Freundlich equation [7], when it is used, as in this case, to describe the equilibrium between a *solid* particle and a *liquid*.

By virtue of the ionization of surface sites or adsorption of ions from the solution, a colloidal particle will develop an electrostatic potential, ϕ , and a surface charge density, $\sigma(\phi)$. If the charge density distribution on the colloidal particle is spherically

symmetric, then the form of $\sigma(\phi)$ can be derived from the electrostatic potential function that satisfies the spherically symmetric Poisson–Boltzmann equation [10],

$$\frac{1}{r} \frac{d^2}{dr^2} (r\Phi(r)) = \frac{-1}{\varepsilon\varepsilon_0} \sum_{i=1}^N Z_i e c_i \exp(-Z_i e \Phi(r)/k_B T), \quad r \geq a \tag{9}$$

In Eq. 9, $\Phi(r)$ is the value of the potential exterior to the particle at a radial distance, r , from its center, ε is the relative dielectric constant of the solution, ε_0 is the dielectric constant of free space, and e is the magnitude of the electron charge. In constructing the sum on the right-hand side, it is assumed that the i -th of the N different ionic species in the solution has volume concentration, c_i . In the Debye–Hückel approximation, where $(Z_i e \phi/k_B T) \ll 1$, Eq. 9 is satisfied by [10]

$$\Phi(r) = \frac{q}{4\pi\varepsilon\varepsilon_0(1 + \kappa a)} \frac{\exp(-\kappa(r - a))}{r} \tag{10}$$

where $q = 4\pi a^2 \sigma$ is the total charge on the colloidal particle, and

$$\kappa^2 = 2e^2 I / \varepsilon\varepsilon_0 k_B T \tag{11}$$

defines the Debye length, $1/\kappa$. In Eq. 11, the ionic strength is

$$I = (1/2) \sum_{i=1}^N Z_i^2 c_i \tag{12}$$

If we equate the total charge outside the solid particle to $-q$, we find that the charge density on the surface of the particle is given by

$$\sigma(\phi) = \varepsilon\varepsilon_0(1 + \kappa a)\phi/a \tag{13}$$

where $\phi = \Phi(a)$ is the value of the electrostatic potential at the surface.

After substitution of Eq. 13 into Eq. 1, we obtain for the interfacial tension,

$$\gamma(a) = \gamma_0 + \Gamma_S k_B T \ln(1 - \theta(\sigma)) - \frac{a\sigma^2}{2\varepsilon\varepsilon_0(1 + \kappa a)} \tag{14}$$

We note the fact that the functional form of $\gamma(a)$ in Eq. 14 satisfies the limits, $\lim_{a \rightarrow \infty} (\gamma(a)/a) = \lim_{a \rightarrow \infty} (d\gamma(a)/da) = 0$, which were used to derive Eqs. 7 and 8. Upon substitution of Eq. 14 into Eq. 8, we obtain

$$\ln \left(\frac{m(a)}{m(\infty)} \right) = \frac{2v}{\omega k_B T a} \left[\gamma_0 + \Gamma_S k_B T \ln(1 - \theta(\sigma)) - \frac{a\sigma^2(3 + 2\kappa a)}{4\varepsilon\varepsilon_0(1 + \kappa a)^2} \right] \tag{15}$$

Equation 15 determines the size dependence of the solubility of a charged colloidal particle that is in equilibrium with an electrolyte solution. As such, it can be used as the basis for a theory of coarsening of crystal sizes by Ostwald ripening.

2.3 Capillary Length Scale

When $\Gamma_S = 0$ and $\sigma = 0$, the right-hand side of Eq. 15 reduces to the form $\ln(m(a)/m(\infty)) = (\alpha/a)$, in which $\alpha = 2v\gamma_0/\omega k_B T$ is known as the *capillary length* [11]. When $\Gamma_S \neq 0$ and $\sigma \neq 0$, the electrostatic term in Eq. 15 becomes independent of a when $\kappa a \gg 1$. In this limit, we can define the capillary length scale,

$$\alpha = \frac{2v\gamma'_0}{\omega k_B T} \quad (16)$$

where

$$\gamma'_0 = \gamma_0 + \Gamma_S k_B T \ln(1 - \theta(\sigma)) - \frac{\sigma^2}{2\epsilon\epsilon_0\kappa} \quad (17)$$

By virtue of the fact that the second and third terms on the right-hand side of Eq. 17 are both negative, γ'_0 is less than γ_0 , and one may regard Eq. 16 as the definition of a “reduced” capillary length, α . The asymptotic nature of Ostwald ripening theory requires $a \gg \alpha$ [6]. We will show that this restriction is ordinarily satisfied, if $\kappa a \gg 1$.

2.4 Theory of Ostwald Ripening

When the solution phase is sufficiently dilute in solute, one can replace the time-dependent molality, $m(t)$, by the time-dependent volume concentration, $c(t) = \rho m(t)/N_A$, where ρ is the mass density of the solution, and N_A is the Avagadro number. The supersaturation, $\Delta(t)$, that drives the coarsening process is then defined by

$$\Delta(t) = \frac{c(t) - c(\infty)}{c(\infty)} \quad (18)$$

Here $c(\infty)$ is the long-time value of the concentration, or what is the same thing, the solubility of the bulk solid. The initial value of the supersaturation, $\Delta(0)$, is obtained by substituting $c(0)$ into Eq. 18. Following Marqusee and Ross [6], we define the volume scale factor, K , as

$$K = \frac{4\pi\alpha^3}{3vc(\infty)} \quad (19)$$

At time t , we let the number of precipitate grains per unit volume be $N(t)$, and the average particle radius in the distribution of particle sizes be denoted by $\langle a(t) \rangle$.

In the theory of Ostwald ripening, one ordinarily distinguishes between two limiting forms for the growth mechanism which are: (a) the rate of growth of a precipitate particle is controlled by the rate of addition of solute molecules to the surface of the particle (interface control) [12] and (b) the rate of growth of the particle is controlled

by the rate of diffusion of solute through the bulk of the solution (diffusion control) [13].

When the particle growth is under *interface control*, the time scale governing the coarsening process is given by [6]

$$T' = \frac{\alpha}{kc(\infty)} \tag{20}$$

where k is the rate constant for addition of molecules to the surface of the particle. In this case, the time-dependent functions governing the supersaturation, the particle density, and the average particle radius are, respectively [6],

$$\Delta(t) = (2T'/t)^{1/2} \approx (\alpha/t)^{1/2} \tag{21a}$$

$$N(t) = 2.96 \frac{\Delta(0)}{K} \left(\frac{T'}{t}\right)^{3/2} \approx \frac{1}{(\alpha t)^{3/2}} \tag{21b}$$

$$\langle a(t) \rangle = 0.629\alpha \left(\frac{t}{T'}\right)^{1/2} \approx (\alpha t)^{1/2} \tag{21c}$$

On the basis of Eqs. 21, which apply in the case of interface control, we conclude that for a fixed time, t , the supersaturation decays faster, and the crystals are smaller in size and greater in number as the capillary length scale, α , decreases.

When the particle growth is under *diffusion control*, the time scale for the coarsening process is given by [6]

$$T'' = \frac{\alpha^2}{Dvc(\infty)} \tag{22}$$

where D is the solute diffusion coefficient. In this case, the time dependent functions governing the supersaturation, the particle density, and the average particle radius are, respectively [6],

$$\Delta(t) = 1.31(T''/t)^{1/3} \approx (\alpha^2/t)^{1/3} \tag{23a}$$

$$N(t) = 1.99 \frac{\Delta(0)}{K} \left(\frac{T''}{t}\right) \approx \frac{1}{\alpha t} \tag{23b}$$

$$\langle a(t) \rangle = 0.763\alpha \left(\frac{t}{T''}\right)^{1/3} \approx (\alpha t)^{1/3} \tag{23c}$$

On the basis of Eqs. 23, which apply in the case of diffusion control, we can conclude that for a fixed time, t , the supersaturation decays faster, and the crystals are smaller in size and greater in number as the capillary length scale, α , decreases. Thus, the qualitative effect of the reduced capillary length is the same under *diffusion control* as it is under *interface control*.

3 Discussion and Conclusions

The Debye–Hückel approximation limits to a certain extent that the size of the electrostatic term, $\sigma^2/2\varepsilon\varepsilon_0\kappa$, in Eq. 17 that we can consider; nonetheless, it is still possible within this approximation to assess the role of the double layer for some representative crystals when they are suspended in 1–1 electrolytes. For a 1–1 electrolyte ($|Z_1| = |Z_2| = 1$) at $T = 298$ K, the Debye–Hückel approximation requires $\phi < k_B T/e = 26$ mV. In the case of water at this temperature, we can set $\varepsilon = 78.54$ and convert Eq. (11) to the numerical form,

$$\kappa = 3.29 \times 10^9 \text{ m}^{-1} \cdot \text{L}^{1/2} \cdot \text{mol}^{-1/2} \sqrt{I(\text{mol} \cdot \text{L}^{-1})} \quad (24)$$

At an ionic strength, $I = 0.05$ M, we find on the basis of Eq. 24 that $\kappa = 7.35 \times 10^8 \text{ m}^{-1}$. For a particle of radius $a = 100$ nm, the product $\kappa a = 73.5$. A surface charge density of $|\sigma| = 1 \mu\text{C} \cdot \text{cm}^{-2}$ is typical of the crystals of many substances [1, 14]. With $\sigma = 1 \mu\text{C} \cdot \text{cm}^{-2}$, $a = 100$ nm, and $\kappa = 7.35 \times 10^8 \text{ m}^{-1}$, Eq. 13 predicts $\phi = 19.3$ mV, which is well within the Debye–Hückel limit. Under these conditions, the electrostatic term in Eq. 17 is $\sigma^2/2\varepsilon\varepsilon_0\kappa = 0.1 \text{ mJ} \cdot \text{m}^{-2}$. For the purpose of comparing theory with experiment, we now turn to specific examples, which include silver iodide and various protein crystals.

The quintessential colloid forming inorganic substance is AgI [14]. Since the solubility of AgI in water at 298 K is only 1.2×10^{-8} M [15], maintenance of an ionic strength of $I = 0.05$ M depends upon the addition of inert electrolyte. Since AgI is a salt, $\Gamma_S = 0$, which means that the chemical term on the right-hand side of Eq. 17 can be ignored. When it comes to assigning a numerical value to γ_0 , however, we are faced with the famously difficult problem of defining the interfacial tension of a solid [16]. We observed that despite this ambiguity, interfacial tension values for the lower molar mass silver halides have been estimated by fitting the measured growth rates of their crystals to one or more crystal growth rate theories [17]. Although the interfacial tension of AgI has yet to be evaluated in this way, we can on the basis of the downward trend in interfacial tension, which occurs with increasing silver halide molar mass, choose $\gamma_0 = 32.5 \text{ mJ} \cdot \text{m}^{-2}$ for AgI. By comparison, our estimate of $0.1 \text{ mJ} \cdot \text{m}^{-2}$ for the electrostatic term in Eq. 17 is *less than 1%* of $\gamma_0 = 32.5 \text{ mJ} \cdot \text{m}^{-2}$. This leads us to the conclusion that the capillary length scale for AgI is little affected by the presence of the double layer. On the basis of the formula weight ($234.77 \text{ g} \cdot \text{mol}^{-1}$) and crystal density ($5.67 \text{ g} \cdot \text{cm}^{-3}$), the molecular volume for AgI is $v = 6.88 \times 10^{-23} \text{ cm}^3$. Since AgI is a 1–1 electrolyte, the sum of the stoichiometric coefficients is $\omega = 2$. If we ignore the chemical and electrostatic terms in Eq. 17, we can use these data and Eq. 16 to compute $\alpha = 0.5$ nm. The restriction, $a \gg \alpha$, is thus well satisfied by a particle with radius equal to 100 nm.

A surface charge density of $\sigma = 1 \mu\text{C} \cdot \text{cm}^{-2}$ is also typical of protein crystals [18]. For the protein crystals, however, the reported interfacial tension values, which depend upon the crystal facet, are two orders of magnitude smaller than our estimate of the interfacial tension for AgI. Since the theory of Ostwald ripening assumes the interfacial tension to be isotropic, we choose for each protein crystal one of the facets

to be representative of the crystal as a whole. In order to make the most stringent comparison between the electrostatic term in Eq. 17 and experiment, we have selected the crystal facet with the largest value of the interfacial tension to serve as an upper bound for the crystal. On this basis, we consider the interfacial tension to be equal to $0.2 \text{ mJ} \cdot \text{m}^{-2}$ for apoferritin [19], $0.32 \text{ mJ} \cdot \text{m}^{-2}$ for catalase [20], and $0.4 \text{ mJ} \cdot \text{m}^{-2}$ for thaumatin [20]. Again assuming $I = 0.05 \text{ M}$, the electrostatic term equals $0.1 \text{ mJ} \cdot \text{m}^{-2}$. As this value is of the same order of magnitude as our upper bounds, the double layer must play a substantial role in determining the interfacial tension of a protein crystal.

Moreover, because protein crystals are molecular solids where the exchangeable ion species, presumably H^+ [21], is bound to various Bronsted–Lowry acid/base sites along the macromolecular chain, we cannot ignore the chemical contributions to the interfacial tension. As there are as many as eight types of Bronsted–Lowry, acid/base functional groups in most proteins [22], the single chemical term in Eq. 17 should be replaced by a sum that includes terms representing the ionizations of the various amino acid residues.

The combined effect in Eq. 17 of the chemical and electrostatic terms, which are both negative, may be sufficient in the case of some proteins to nearly cancel the term, γ_0 , that determines the interfacial tension of the uncharged surface. Near cancellation would lead to a reduced value for the capillary length, which we suggest may explain the fact that the supersaturation in a typical protein crystallization experiment requires a few days to reach equilibrium [18,23], while the crystals that appear are ordinarily less than $50 \mu \text{ m}$ on a side [21,24].

Because of the mix of positive and negative terms on the right-hand side of Eq. 15, there may exist for certain conditions of supersaturation a value of the radius, $a = a_m$, where $\ln(m(a)/m(\infty))$ assumes a minimum. Under these conditions, which are currently under investigation, small crystals with radii $a < a_m$ should grow, while larger crystals with radii $a > a_m$ should dissolve. Over time, both groups of crystals should presumably approach some limiting radius determined by the value of a_m . Finally, in order to relax the restriction placed on the theory by the Debye–Hückel approximation, we note that the Poisson–Boltzmann equation can be solved for larger values of the surface potential, ϕ , using one of the available numerical [25] or approximate analytical [26] methods.

References

1. W. Stumm, J.J. Morgan, *Aquatic Chemistry* (John Wiley, New York, 1981), Chap. 10
2. D.Y.C. Chan, D.J. Mitchell, *J. Colloid Interface Sci.* **95**, 193 (1983)
3. J.Th.G. Overbeek, *Colloid Surf.* **51**, 61 (1990)
4. M. Manciu, E. Rukenstein, *Langmuir* **19**, 1114 (2003)
5. W. Wu, G.H. Nancollas, *J. Colloid Interface Sci.* **182**, 365 (1996)
6. J.A. Marqusee, J. Ross, *J. Chem. Phys.* **79**, 373 (1983)
7. R. Defay, I. Prigogine, A. Bellemans, *Surface Tension and Adsorption* (John Wiley, New York, 1966)
8. R.A. Robinson, R.H. Stokes, *Electrolyte Solutions* (Butterworths, London, 1959), pp. 24–28
9. A. Frenkel, *J. Chem. Phys.* **7**, 538 (1939)
10. R.S. Berry, S.A. Rice, J. Ross, *Physical Chemistry* (John Wiley, New York, 1980), pp. 998–1000
11. R. Finsy, *Langmuir* **20**, 2975 (2004)
12. C. Wagner, *Z. Electrochem.* **65**, 581 (1961)
13. I.M. Lifshitz, V.V. Slyozov, *J. Phys. Chem. Solids* **19**, 35 (1961)

14. J. Lyklema, *Adv. Colloid Interface Sci.* **100**, 1 (2003)
15. P.W. Atkins, *Physical Chemistry*, 4 edn. (W. H. Freeman and Company, New York, 1990), p. 955
16. J.S. Rowlinson, B. Widom, *Molecular Theory of Capillarity* (Clarendon Press, Oxford, 1982), p. 8
17. A.E. Nielsen, O. Sohnel, *J. Cryst. Growth* **11**, 233 (1971)
18. Y.W. Kim, D.A. Barlow, K.G. Caraballo, J.K. Baird, *Mol. Phys.* **101**, 2677 (2003)
19. S.-T. Yau, P.G. Vekilov, *Nature* **406**, 494 (2000)
20. A.J. Malkin, Yu.G. Kuznetsov, A. McPherson, *J. Cryst. Growth* **196**, 471 (1999)
21. A.M. Holmes, S.G. Holliday, J.C. Clunie, J.K. Baird, *Acta Cryst. D* **D53**, 456 (1997)
22. J.K. Baird, Y.W. Kim, *Mol. Phys.* **100**, 1855 (2002)
23. K.G. Caraballo, J.K. Baird, J.D. Ng, *Cryst. Growth Des.* **6**, 874 (2006)
24. H.-M. Lee, Y.W. Kim, J.K. Baird, *J. Cryst. Growth* **232**, 294 (2001)
25. B.J. Yoon, *J. Colloid Interface Sci.* **192**, 503 (1997)
26. S. Zhou, *J. Colloid Interface Sci.* **208**, 347 (1998)